Transport of dense colloids in porous media

Constantinos V. Chrysikopoulos[1], Vasileios E. Katzourakis[2] & Vasiliki I. Syngouna[2]

(1) School of Environmental Engineering, Technical University of Crete, Chania, Greece, e-mail: cvc@enveng.tuc.gr
(2) Department of Civil Engineering, University of Patras, Patras, Greece, e-mails: billiskatz@yahoo.gr & kikisyg@yahoo.gr

Abstract: The role of gravitational force on dense-colloid transport in porous media was investigated. Transport experiments were performed with colloids in columns packed with glass beads placed in various orientations (horizontal, vertical, and diagonal). All experiments were conducted under electrostatically unfavorable conditions. The experimental data were fitted with a newly developed, analytical, one-dimensional, colloid transport model. The effect of gravity is incorporated in the mathematical model by combining the interstitial velocity (advection) with the settling velocity (gravity effect). The results revealed that flow direction influences colloid transport in porous media. The rate of particle deposition was shown to be greater for up-flow than for down-flow direction, suggesting that gravity was a significant driving force for colloid deposition. Furthermore, a three-dimensional numerical model was developed to investigate the simultaneous transport (cotransport) of dense colloids and viruses in homogeneous, water saturated, porous media with horizontal uniform flow. The dense colloids are assumed to exist in two different phases: suspended in the aqueous phase, and attached reversibly or irreversibly onto the solid matrix. The viruses are assumed to exist in four different phases: suspended in aqueous phase, attached onto the solid matrix, attached onto suspended colloids, and attached onto colloids already attached onto the solid matrix. The governing differential equations were solved numerically with the finite difference schemes, implicitly or explicitly implemented so that both stability and speed factors were satisfied. Model simulations have shown that the presence of dense colloid particles can either enhance or hinder the horizontal transport of viruses, but also can increase the vertical migration of viruses.

Key words: gravity effects, clay minerals, KGa-1b, STx-1b, colloid transport

1. INTRODUCTION

The transport of colloids in porous and fractured media has long been recognized to be of considerable importance to a number of environmental practical applications, including groundwater pollution by microbial pathogens, in situ bioremediation of contaminated aquifers, and granular filtration of water and wastewater. Numerous investigators have examined theoretically and experimentally the various factors that affect colloid transport in porous and fractured media, especially the effects of interstitial velocity, colloid particle size,[5-9] collector size,[10-12] solid matrix porosity,[13] collector roughness,[9,14-16] ionic strength,[17] water chemistry,[21-23] gravitational settling,[24-26] and presence of suspended clays.[29-32]

The effect of flow direction on colloid fate and transport in porous media has received relatively minor attention. However, laboratory experiments with bench-scale model aquifers are traditionally conducted with flow direction orthogonal to gravity (horizontal flow),[33-35] whereas packed column experiments are carried out with flow orthogonal to gravity,[30,31,36] against gravity (up-flow),[7,23] or in the direction of gravity (down-flow).[43-45] The up-flow direction is widely used because packed columns are traditionally saturated using up-flow to reduce air entrapment. However, numerous of the published studies do not report the flow direction used, and either neglect or regard insignificant the influence of gravitational settling, which is potentially a significant retention mechanism.

Furthermore many pollutants, including biocolloids, in aqueous media are readily adsorbed/attached onto colloidal particles, which often act as carriers. Several experimental and theoretical studies have shown that, depending on the physicochemical conditions of the fractured and porous media, colloids can either enhance or hinder the transport of organic and inorganic pollutants[1-3]. Multiple research groups have developed analytical and numerical mathematical models to describe and predict colloid and biocolloid transport in fractured and porous media[4,18,48]. Although there are numerous mathematical models available that describe colloid transport in porous media, in this study, the frequently employed continuum approach was adopted. The phenomenological colloid transport model developed by Sim and Chrysikopoulos[46] was extended firstly to account for colloid sedimentation, in order to examine how the flow direction influences colloid fate and transport in porous media and secondly to account for colloid-facilitated virus transport in three-dimensional, water saturated, homogeneous porous media with uniform flow. To our knowledge, clay mineral

transport in columns packed with glass beads under various flow directions, and electrostatically unfavorable conditions has not been previously explored.

2. MATHEMATICAL DEVELOPMENT

2.1 One Dimensional Transport of Dense Colloids

Based on the continuum approach, the transport of colloids (including biocolloids) in one-dimensional, homogeneous, water saturated porous media with first-order attachment (or filtration) and inactivation, assuming that an effective velocity term accounts for both the interstitial as well as the particle settling velocity is governed by the following partial differential equation:

$$\frac{\partial C(t,x)}{\partial t} + \frac{\varrho_b}{\theta}\frac{\partial C^*(t,x)}{\partial t} = D\frac{\partial^2 C(t,x)}{\partial x^2} - U_{tot}\frac{\partial C(t,x)}{\partial x} - \lambda C(t,x) - \lambda\frac{\varrho_b}{\theta}C^*(t,x) \quad (1)$$

where C [M/L^3] is the concentration of colloids in suspension; C* [M/M] is the concentration of colloids attached on the solid matrix; t [t] is time; ρ_b [M/L^3] is the bulk density of the solid matrix; θ [-] is the porosity of the porous medium; D [L^2/t] is the hydrodynamic dispersion coefficient; λ [1/t] is the transformation rate constant of suspended colloids (e.g., inactivation, which refers to loss of infective capability or die-off of suspended biocolloids); λ* [1/t] is the transformation rate constant of colloids attached on the solid matrix; and U_{tot} [L/t] is the total (or effective) particle velocity, which for colloids subject to gravitational forces accounts for gravitational settling:

$$U_{tot} = U + U_{s(i)} \quad (2)$$

where U [L/t] is the interstitial velocity, and $U_{s(i)}$ [L/t] is a modified version of the traditional "free particle" settling velocity in static water columns,[47] to "restricted particle" settling in granular porous media under directional flow conditions:

$$U_{s(i)} = -f_s\frac{(\varrho_p - \varrho_w)\, d_p^2}{18\mu_w} g_{(i)} \quad (3)$$

where f_s [-] is the correction factor accounting for particle settling in the presence of the solid matrix of granular porous media, ρ_w [M/L^3] and ρ_p [M/L^3] are the densities of the suspending fluid (water) and the colloid particle, respectively; μ_w [M/(L·t)] is the dynamic viscosity of water, and $g_{(i)}$ [L/t^2] is the gravity vector along the direction of the interstitial flow defined as:

$$g_{(i)} = g_{(-z)}\sin\beta\ \mathbf{i} \quad (4)$$

where $g_{(-z)}$ [M/t^2] is the acceleration due to gravity in the negative z-direction (indicated by the subscript in parentheses), β [°] is the angle of the main flow direction with respect to the horizontal x-direction, and **i** is the unit vector parallel to the flow. For up-flow $0°<\beta<90°$, whereas for down-flow $-90°<\beta<0°$. Furthermore, it should be noted that for the case of diagonal (or inclined) orientation, although the gravity vector component $g_{(i)}=g_{(-z)}\sin\beta$ **i**, is accounted for in the one-dimensional model as gravity effect, the vector component $g_{(-j)}=-g_{(-z)}\cos\beta$ **j**, is not necessarily balanced and can cause colloid deposition or lateral dispersion. The vector component $g_{(-j)}$ cannot be considered in the one-dimensional model used in this study.

The correction factor f_s [-] converts the average free particle sedimentation velocity to the average sedimentation velocity through water saturated porous media:[24]

$$f_s = \frac{b + 0.67}{b + 0.93/\varepsilon} \quad (5)$$

where b represents the ratio of the average free settling segment length to the grain radius, and ε [-] ($0\le\varepsilon\le1$) is an empirical correction factor arising from influences of the grain surface. It should be noted that $f_s\approx0.9$ when the grains of the granular porous media contribute only to tortuosity and do not provide additional frictional resistance.[24]

It should be noted that the governing colloid transport equation (1) is essentially the colloid transport model provided by Sim and Chrysikopoulos[46] with U replaced by U_{tot}. Also, (3) is the

balance among gravity, buoyancy and viscous forces, implicitly assumes that the colloids are small, uniform spheres, and there is a distinct density difference between the colloids and the suspending fluid. The rate of colloid attachment onto the solid matrix is described by the following first-order equation:[41]

$$\frac{\varrho_b}{\theta}\frac{\partial C^*(t,x)}{\partial t} = k_c C(t,x) - k_r \frac{\varrho_b}{\theta} C^*(t,x) - \lambda^* \frac{\varrho_b}{\theta} C^*(t,x) \quad (6)$$

where k_c [1/t] is the attachment rate constant, and k_r [1/t] is the detachment rate constant.

The initial and boundary conditions employed are:

$$C(0,x) = 0 \quad (7)$$

$$D\frac{\partial C(t,0)}{\partial x} + U_{tot} C(t,0) = \begin{cases} U_{tot} C_0 & 0 < t \le t_p \\ 0 & t > t_p \end{cases} \quad (8)$$

$$\frac{\partial C(t,\infty)}{\partial x} = 0 \quad (9)$$

where C_0 [M/L^3] is the source concentration of colloids suspended in the aqueous phase, and t_p [t] is the colloid broad pulse duration. The first condition (7) states that porous medium is initially free of colloids. Condition (8) is a typical constant flux boundary condition, which implies concentration discontinuity at the inlet of the porous medium.[42] Condition (9) describes that a concentration-continuity is preserved at the downstream boundary of the semi-infinite porous medium. The analytical solution to the partial differential equations (1) and (6), subject to the initial and boundary conditions (7)-(9), with U instead of U_{tot}, has been derived by Sim and Chrysikopoulos.[46]

It should be noted that the present colloid transport model is different from traditional models only in the velocity term, U_{tot}, which is essentially an effective velocity and accounts for both the interstitial velocity as well as the free particle settling velocity. The various model parameters can be estimated by fitting the analytical solution to the experimental data with the nonlinear least squares regression package "ColloidFit,"[46] which can be obtained for free from the authors upon request.

2.2 Three Dimensional Transport of Dense Colloids

The proposed colloid facilitated virus transport model assumes that the colloids partition between the aqueous phase and the solid matrix, while viruses may attach onto colloidal particles in the aqueous phase, onto the solid matrix, and onto colloids previously attached onto the solid matrix. Consequently, colloid particles can be suspended in the aqueous phase C_c [M_c/L^3], or attached onto the solid matrix C_{c^*} [M_c/M_s]. Viruses can be suspended in the aqueous phase C_v [M_v/L^3], directly attached onto the solid matrix C_{v^*} [M_v/M_s], attached onto suspended colloid particles (virus-colloid particles) C_{vc} [M_v/M_c], and attached onto colloid particles already attached onto the solid matrix (or equivalently virus-colloid particlsfes attached onto the solid matrix) $C_{v^*c^*}$ [M_v/M_c]. To simplify the notation, the various masses are indicated as follows: M_c is the mass of colloids, M_v is the mass of viruses, and M_s is the mass of the solid matrix. Also, the subscripts c, v, and vc represent colloid, virus and virus-colloid, respectively.

The transport of suspended colloid particles in three-dimensional saturated, homogeneous porous media with uniform flow, accounting for nonequilibrium attachment onto the solid matrix, is governed by the following partial differential equation,[32] which is extended to include gravity terms:

$$\frac{\partial C_c(t,x,y,z)}{\partial t}+\frac{\varrho_b}{\theta}\frac{\partial C_{c^*}(t,x,y,z)}{\partial t}-D_{xc}\frac{\partial^2 C_c(t,x,y,z)}{\partial x^2}-D_{yc}\frac{\partial^2 C_c(t,x,y,z)}{\partial y^2}$$
$$-D_{zc}\frac{\partial^2 C_c(t,x,y,z)}{\partial z^2}+\left(U_x+U_{cs(\pm i)}\right)\frac{\partial C_c(t,x,y,z)}{\partial x}+U_{cs(-k)}\frac{\partial C_c(t,x,y,z)}{\partial z} \qquad (10)$$
$$=F_c(t,x,y,z)$$

where t [t] is time; x [L] is the Cartesian coordinate in the longitudinal direction; y [L] is the Cartesian coordinate in the lateral direction; z [L] is the Cartesian coordinate in the vertical direction; ρ_b [M_s/L^3] is the bulk density of the solid matrix; θ [–] is the porosity of the porous medium; D_{xc}, D_{yc}, D_{zc} [L^2/t] are the longitudinal, lateral, and vertical hydrodynamic dispersion coefficients of the suspended colloids, respectively; F_c [M_c/L^3t] is a general form of the colloid source configuration; U_x [L/t] is the average interstitial velocity along the x-direction; and $U_{cs(\pm i)}$ [L/t] and $U_{cs(-k)}$ [L/t] are the ±x-directional and negative z-directional components of the "restricted particle" settling velocity. The colloid accumulation term is described by the following nonequilibrium equation:[32]

$$\frac{\varrho_b}{\theta}\frac{\partial C_{c^*}(t,x,y,z)}{\partial t}=r_{c\text{-}c^*}C_c(t,x,y,z)-r_{c^*\text{-}c}\frac{\varrho_b}{\theta}C_{c^*}(t,x,y,z) \qquad (11)$$

where $r_{c\text{-}c^*}$ [1/t] is the rate coefficient of the colloid attachment onto the solid matrix, and $r_{c^*\text{-}c}$ [1/t] is the rate coefficient of the colloid detachment from the solid matrix;

The transport of suspended viruses in three-dimensional water saturated porous media, accounting for virus attachment onto (a) the solid matrix, (b) suspended colloid particles, and (c) colloid particles already attached onto the solid matrix, as well as for first-order decay (inactivation) of suspended and attached viruses with different decay rates, is governed by the following partial differential equation,[32] which is extended to include gravity terms:

$$\frac{\partial}{\partial t}(C_v+\frac{\varrho_b}{\theta}C_{v^*}+C_cC_{vc}+\frac{\varrho_b}{\theta}C_{c^*}C_{v^*c^*})=D_{xv}\frac{\partial^2 C_v}{\partial x^2}+D_{xvc}\frac{\partial^2}{\partial x^2}(C_cC_{vc})+D_{yv}\frac{\partial^2 C_v}{\partial y^2}$$
$$+D_{yvc}\frac{\partial^2}{\partial y^2}(C_cC_{vc})+D_{zv}\frac{\partial^2 C_v}{\partial z^2}+D_{zvc}\frac{\partial^2}{\partial z^2}(C_cC_{vc})$$
$$-\left(U_x+U_{vs(\pm i)}\right)\frac{\partial}{\partial x}(C_v+C_cC_{vc})$$
$$-U_{vs(-k)}\frac{\partial}{\partial z}(C_v)-U_{vcs(-k)}\frac{\partial}{\partial z}(C_cC_{vc}) \qquad (12)$$
$$-\lambda_vC_v-\lambda_{vc}C_vC_{vc}-\lambda_{v^*}\frac{\varrho_b}{\theta}C_{v^*}$$
$$-\lambda_{v^*c^*}\frac{\varrho_b}{\theta}C_{c^*}C_{v^*c^*}+F_v(t,x,y,z)$$

where λ_v [1/t] is the decay rate of viruses suspended in the aqueous phase; λ_{v^*}[1/t] is the decay rate of viruses attached onto the solid matrix; λ_{vc} [1/t] is the decay rate of virus-colloid particles suspended in the aqueous phase; $\lambda_{v^*c^*}$ [1/t] is the decay rate of virus-colloid particles attached onto the solid matrix; $U_{vs(-k)}$ [L/t] is "restricted" settling velocity of the viruses; and $U_{vcs(-k)}$ [L/t] is "restricted" settling velocity of the virus-colloid complexes and $F_v(t,x,y,z)$ [M_v/L^3t] is a general form of the viruses source configuration.

The second mass accumulation rate that appears on the left side of (12) is described by the following nonequilibrium relation:[32]

$$\frac{\varrho_b}{\theta}\frac{\partial C_{v^*}(t,x,y,z)}{\partial t} = r_{v\text{-}v^*}C_v(t,x,y,z) - r_{v^*\text{-}v}\frac{\varrho_b}{\theta}C_{v^*}(t,x,y,z) - \lambda_{v^*}\frac{\varrho_b}{\theta}C_{v^*}(t,x,y,z) \quad (13)$$

where $r_{v\text{-}v^*}$ [1/t] is the rate coefficient of virus attachment onto the solid matrix, and $r_{v^*\text{-}v}$ [1/t] is the rate coefficient of virus detachment from the solid matrix.

The third mass accumulation rate that appears on the left side of (12) can be expressed by the following extended equation:[32]

$$\frac{\partial}{\partial t}(C_c C_{vc}) = r_{v-vc}(C_c)^2 C_v - r_{vc-v}(C_c C_{vc}) + \frac{\varrho_b}{\theta}r_{v^*c^*-vc}(C_{c^*}C_{v^*c^*}) - r_{vc-v^*c^*}(C_c C_{vc}) - \lambda_{vc}C_c C_{vc} \quad (14)$$

where r_{v-vc} [L^3/M_c t] is the rate coefficient of virus attachment onto suspended colloid particles; r_{vc-v} [1/t] is the rate coefficient of virus detachment from suspended colloids; $r_{vc-v^*c^*}$ [1/t] is the rate coefficient of virus-colloid particle attachment onto the solid matrix; $r_{v^*c^*-vc}$ [1/t] is the rate coefficient of virus-colloid particle detachment from the solid matrix.

The fourth mass accumulation rate that appears on the left side of (12) can be expressed by the following extended equation:[32]

$$\frac{\varrho_b}{\theta}\frac{\partial}{\partial t}(C_{c^*}C_{v^*c^*}) = \frac{\varrho_b}{\theta}r_{v-v^*c^*}(C_{c^*})^2 C_v - \frac{\varrho_b}{\theta}r_{v^*c^*-v}(C_{c^*}C_{v^*c^*}) + r_{vc-v^*c^*}(C_c C_{vc}) - \frac{\varrho_b}{\theta}r_{v^*c^*-vc}(C_{c^*}C_{v^*c^*}) - \lambda_{v^*c^*}\frac{\varrho_b}{\theta}C_{c^*}C_{v^*c^*} \quad (15)$$

where $r_{v-v^*c^*}$ [L^3/M_ct] is the rate coefficient of virus attachment onto colloids already attached onto the solid matrix. $r_{v^*c^*-v}$ [1/t] is the rate coefficient of virus detachment from virus-colloid particles attached onto the solid matrix.

2.3 Initial and boundary conditions

The initial condition and the appropriate boundary conditions for a three-dimensional confined aquifer with finite dimensions are as follows:

$$C_i(0,x,y,z) = 0 \quad (16)$$

$$-D_{xi}\frac{\partial C_i(t,0,y,z)}{\partial x} + UC_i(t,0,y,z) = \begin{cases} UC_{oi}, & t \le t_p \\ 0, & t > t_p \end{cases} \quad (17)$$

$$\frac{\partial C_i^2(t,L_x,y,z)}{dx^2} = 0 \quad (18)$$

$$\frac{\partial C_i(t,x,0,z)}{\partial y} = \frac{\partial C_i(t,x,L_y,z)}{\partial y} = 0 \quad (19)$$

$$\frac{\partial C_i(t,x,y,0)}{\partial z} = \frac{\partial C_i(t,x,y,L_z)}{\partial z} = 0 \quad (20)$$

where the subscript i represents either viruses (i=v) or clay colloids (i=c); L_x, L_y, L_z, [L] are the length, width, and height of the porous medium, respectively; C_{oi} is the initial constant aqueous phase concentration of species i (virus or colloids), and t_p [t] is the time period over which colloids and viruses are injected (inserted) in the porous medium.

2.4 Three dimensional model solution strategy

The unknown variables of the numerical model presented are six: C_c, C_{c^*}, C_{vc}, $C_{v^*c^*}$, C_v and C_{v^*}. To explicitly solve for all six unknowns, a six by six system of equations must be formed, which rapidly increases the required matrix size and thus the number of calculations. However, in this study an alternative procedure was employed. Three sets of equations, consisting of two by two systems of equations, where formed, which were solved in an iterative manner. Note that the two solution procedures produce exactly the same results, but the proposed alternative procedure provides greater speed with lower memory requirements. The systems were solved as follows: (i) Equations (10), (11) where solved simultaneously by the semi implicit Crank-Nicolson method in order to determine C_c, and C_{c^*}. (ii) These C_c and C_{c^*} concentrations were used in (12) and (13), which were solved together with the Pardiso solver in order to get initial estimates for C_v and C_{v^*}. (iii) The estimates C_v and C_{v^*} along with the previously calculated C_c and C_{c^*}, were used in the system of coupled equations (14) and (15), which was solved with the Intel® ode solver to obtain initial estimates for C_{vc} and $C_{v^*c^*}$. (iv) The estimated C_{vc} and $C_{v^*c^*}$ values where fed back to step (ii) in order to produce better estimates for C_v and C_{v^*}, which in turn where employed in step (iii) to improve C_{vc} and $C_{v^*c^*}$ estimates. (v) Steps (ii) through (iv) where repeated till all of the C_{vc}, $C_{v^*c^*}$, C_v and C_{v^*} values provided by successive iterations did not differ more than 5%.

The above steps were repeated sequentially until all unknown concentrations were calculated for the required time period. It should also be noted that for the numerical simulations presented in this study, each physical model was discretized into a number of cells, nx, which was kept as low as possible to produce fast solutions, but high enough to allow for a quite small relative error (1-5%).

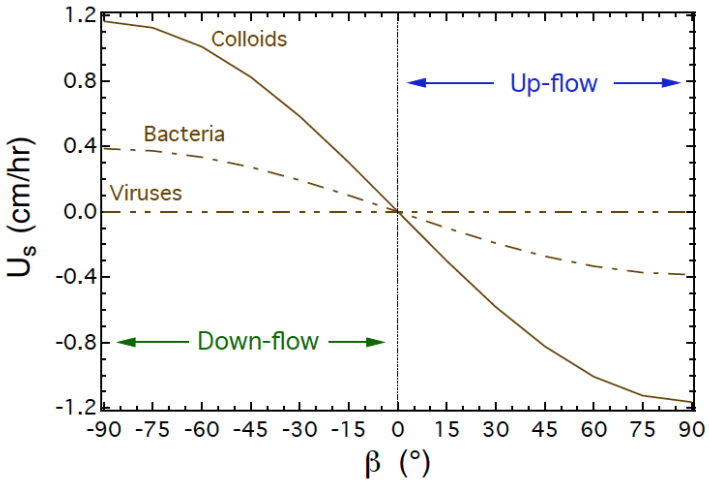

Figure 1. Restricted particle settling velocity as a function of column orientation and flow direction for colloids (clay: d_p=2 μm, ρ_p=2.65 g/cm^3), bacteria (P. putida: d_p=2.2 μm, ρ_p=1.45 g/cm^3), and viruses (bacteriophage MS2: d_p=25 nm, ρ_p=1.42 g/cm^3). Here f_s=0.9.

2.6 Model Simulations

To illustrate the effect of gravity on restricted particle settling in porous media, equation (3) was plotted in Figure 1 as a function of the angle of the main flow direction for both down-flow and up-flow directional flow conditions for hypothetical, relatively dense colloid particles, bacteria and viruses. It should be clarified here that the restricted particle settling is affected by particle size but

also by particle density. Therefore, as shown in Figure 1, the restricted particle settling of colloids and bacteria is affected by gravity, but the settling of small virus particles is practically unaffected by gravity. As expected, $U_{s(i)}$ is positive for down-flow conditions and negative for up-flow conditions; whereas, for horizontal flow $U_{s(i)}=0$. Consequently, $U_{tot}>U$ for down-flow conditions, $U_{tot}<U$ for up-flow conditions, and $U_{tot}=U$ for horizontal flow.

The model simulations presented in Figure 2 indicate that flow direction can significantly affect the transport of dense and/or large colloids. Clearly, there is faster breakthrough for down-flow (see Figure 2a), and lower peak colloid concentrations at the column exit for up-flow (see Figure 2b).

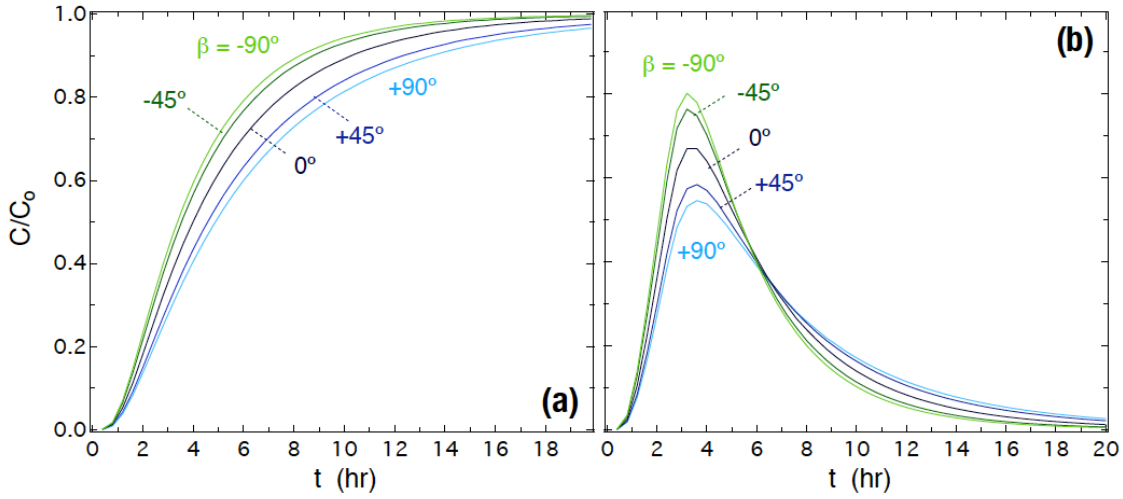

Figure 2. Simulations of normalized colloid break through curves for packed columns with various orientations and flow directions under: (a) continuous, and (b) broad pulse inlet boundary conditions. Here U=4 cm/hr, D=22.5 cm^2/hr, θ=0.45, ρ_b=1.63 g/cm^3, $\lambda=\lambda^*$=0 hr^{-1}, $k_c=k_r$=0 hr^{-1}, x=15 cm, d_p=5 μm, ρ_p=1.15 g/cm^3, and t_p=2 hr.

3. EXPERIMENTAL APPROACH

3.1 Clay colloids

The clays used in this study were kaolinite (KGa-1b, is a well-crystallized kaolin from Washington County, Georgia),[37] and montmorillonite (STx-1b, a Ca-rich montmorillonite, white, from Gonzales County, Texas), purchased from the Clay Minerals Society, Columbia, USA. KGa-1b has a specific surface area of 10.1 m^2/g, and a cation exchange capacity of 2.0 meq/100 g.[38] STx-1b has a specific surface area of 82.9 m^2/g,[39] and assuming that the characteristics of STx-1b are comparable to those of STx-1, which is the previous batch of montmorillonite from the same area, its cation exchange capacity is 84.4 meq/100 g.[38] The <2 μm colloidal fraction was collected and purified as described in Rong et al.[40] The hydrodynamic diameters of the clay particles, were determined by the zetasizer to be d_p=843±126 nm for KGa-1b, and d_p=1187±381 nm for STx-1b.[31] The optical density of the clay colloids was analyzed at a wavelength of 280 nm by a UV-vis spectrophotometer, and the corresponding clay concentrations were determined twice as outlined by Chrysikopoulos and Syngouna.[27] The colloid suspensions were prepared in high-purity distilled deionized Milli-Q water (ddH2O) with specific conductivity of 0.055 μS/cm, ensuring that the pH is close to neutral, which actually ranged between 6.7 and 7. The electrokinetic features (zeta potentials) of the clay colloid suspensions in ddH2O are unfavorable to deposition (negative zeta potentials, high DLVO energy barriers) at pH>2.1.[27]

3.2 Column Experiments

Flow through experiments were carried out with KGa-1b and STx-1b clays as model colloids in a 2.5 cm diameter and 30 cm long Chromaflex glass column packed with 2 mm in diameter glass beads (Fisher Scientific, New Jersey). Glass beads were chosen as model porous media because they are chemically non-reactive with the solutions used in this study.

Constant flow of sterile ddH_2O at flow rate of Q=1.5 mL/min, corresponding to pore water velocity of U=0.74 cm/min, was maintained through the packed column with a peristaltic pump. For each experiment, three pore volumes of the clay colloid suspension were injected into the packed column, followed by three pore volumes of ddH_2O. Note that the columns were placed horizontally ($\beta=0°$), vertically ($\beta=\pm 90°$), and inclined ($\beta=\pm 45°$). A fresh column was packed for each experiment. Chloride, in the form of potassium chloride, was chosen as the nonreactive tracer for the transport column experiments. One set of flow through experiments was performed with clay colloid transport in horizontal ($\beta=0°$), a second set in vertical ($\beta=\pm 90°$), and a third set in inclined ($\beta=\pm 45°$) columns. For all sets, three pore-volumes of solution were injected into the packed column, followed by three pore volumes of ddH_2O. All experiments were carried out at room temperature (~25°C).

4. RESULTS AND DISCUSSION

The normalized KGa-1b and STx-1b flowthrough experimental data are presented in Figure 3, together with the fitted model predictions. The parameters $U_{tot,}$ D and k_c were estimated with the nonlinear least squares regression package "ColloidFit" by fitting the analytical solution to the experimental KGa-1b and STx-1b breakthrough concentrations. Note that in order to keep the number of the fitted parameters equal to three, it was assumed that k_r, λ, and λ^* are negligible.[4] The fitted parameters $U_{tot,}$ D and k_c together with their corresponding 95% confidence intervals are listed in Table 1. Traditionally, packed column dispersion coefficients are determined from tracer behavior; however, in this study, although tracer experiments were conducted and analyzed, the dispersion coefficient for the colloid transport data collected was treated as a fitted parameter, because colloid dispersivities are significantly different than tracer dispersivities.[7] From the fitted U_{tot} values listed in Table 1, the fitted restricted particle settling velocity was easily obtained as $U_{s(i)}=U_{tot}-0.74$ cm/min, because for all experiments of this study U was fixed at 0.74 cm/min. Note that $U_{s(i)}$ is a function of both colloid size and density.

From Table 1 it is evident that all fitted U_s values followed the theoretical trend suggested by (3) ($U_{s(i)}=0$ for horizontal flow, $U_{s(i)}>0$ for down-flow, and $U_{s(i)}<0$ for up-flow). Based on the fitted k_c values listed in Table 1, particle attachment is generally higher for up-flow than down-flow experiments. This observation is in agreement with the results reported by Basha and Culligan[19] who conducted experiments under unfavorable conditions using smooth as well as rough bead packs, and observed that for down-flow experiments, straining was the primary filtration mechanism in the smooth bead packs, whereas, both straining and attachment by surface asperities were important filtration mechanisms in the rough bead packs, but roughness did not affect significantly the filtration process for up-flow experiments. In contrast, Ma et al.[28] found that colloidal deposition rate constants, under conditions favorable to deposition, were slightly higher for down-flow than up-flow experiments.

Only a fraction of the injected clay colloids was recovered at the column effluent, due to clay colloid deposition onto the glass beads. The calculated mass recovery, M_r, values listed in Table 1 suggested that there was more mass retained in the columns under upward than downward flows. With the exception of KGa-1b with VU mode (see exp. 2 in Table 1), higher mass recoveries were observed for both clays for VD than DD flow directions, and for downward than upward flows. For the same flow conditions, higher retention of KGa-1b than STx-1b was observed (see Table 1), which could be attributed to the higher hydrophobicity of KGa-1b. This observation is in agreement

with previous studies.[27,31] The first normalized temporal moment for each breakthrough curve was calculated with (14) and listed in Table 1. Also, the ratio of the first normalized temporal moment, of the colloid, $M_{1(c)}$ for the two clays (KGa-1b, STx-1b) to $M_{1(t)}$ for the tracer Cl^- was computed for each flow direction employed (see Table 1). It is worthy to note that, with the exception of exp. 7, velocity enhancement ($M_{1(c)}/M_{1(t)}>1$) was observed for both of the clay colloids and all of the flow conditions considered in this study. The observed early breakthrough of the two clays, compared to the conservative tracer, is attributed to size exclusion.[7,20] The relatively large clay particles were excluded from small pores spaces, and sampled the more conductive ranges of the interstitial velocity distribution.[5] Consequently, the clay particles were transported faster than the conservative tracer. Finally, Figure 4 represents an example of 2D cotransport simulation using default parameter values found in literature.[32]

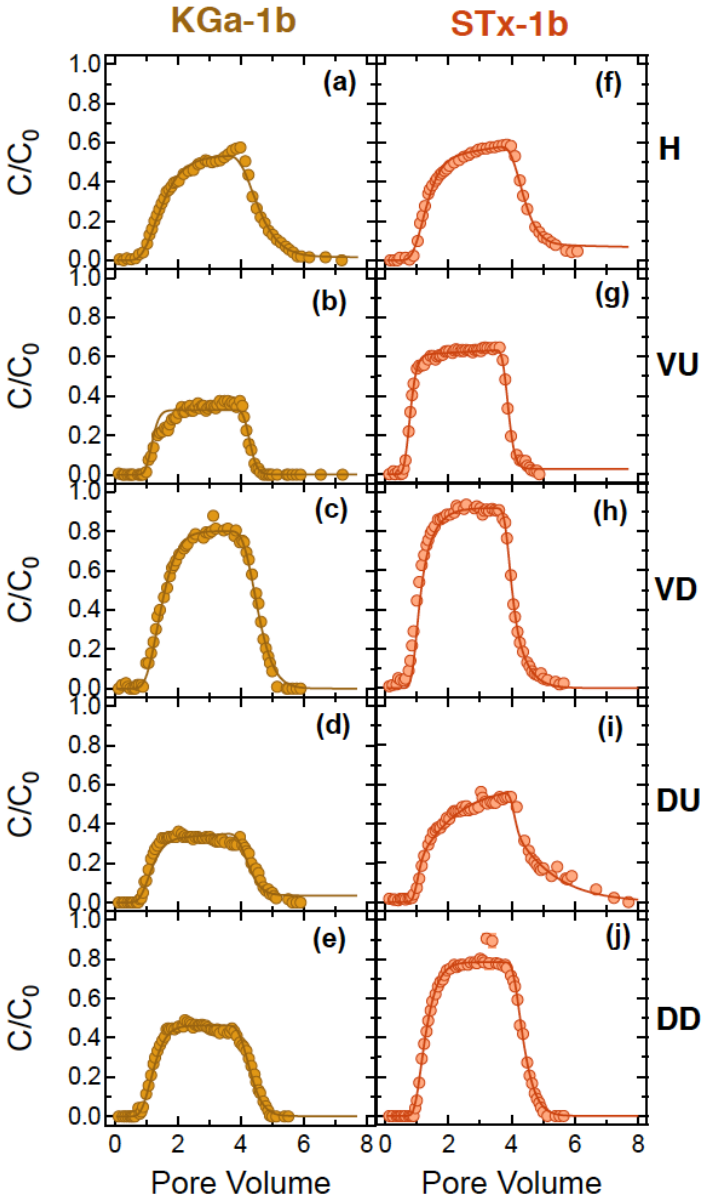

Figure 3. Experimental data (symbols) and fitted model simulations (curves) of (a-e) KGa-1b and (f-j) STx-1b breakthrough in columns packed with glass beads with (a,f) horizontal, (b,g) vertical up-flow, (c,h) vertical down-flow, (d,i) diagonal up-flow, and (e,j) diagonal down-flow directional flow conditions. Here, H-horizontal, VU-vertical up-flow, VD-vertical down-flow, DU-diagonal up-flow, DD-diagonal down-flow.

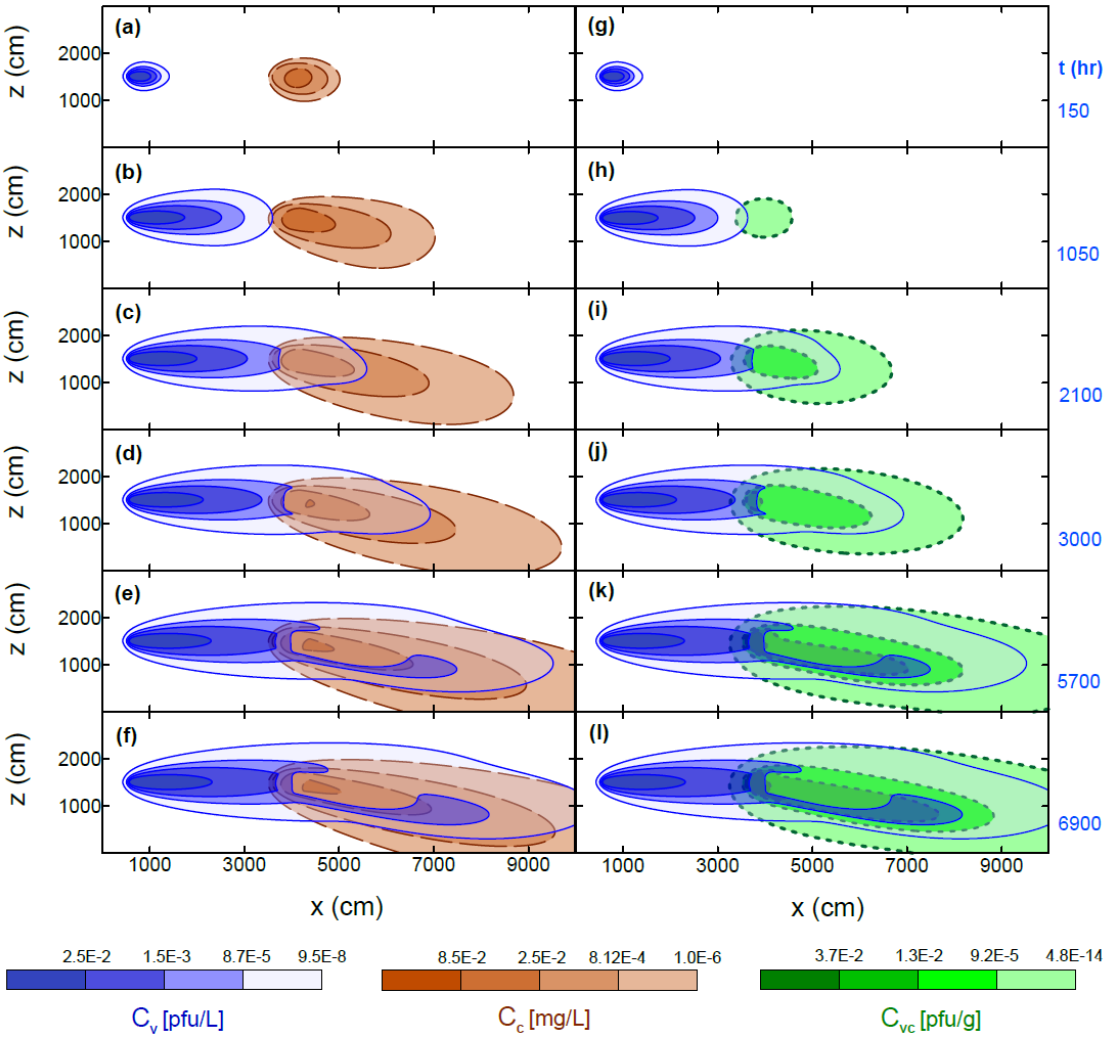

Figure 4. Contour plots on the x-z plane for: (a-f) viruses (solid curves) and colloid particles (dashed curves), and (g-l) viruses (solid curves) and virus-colloid particles (dotted curves) during virus and colloid cotransport in the presence of gravitational effects. Here (a,g) t=150 hr, (b,h) t=1050 hr, (c,i) t=2010 hr, (d,j) t=3000 hr, (e,k) t=5700 hr, (f,l) t=6900 hr, and y=15 m.

Table 1. Experimental conditions, fitted parameter values, and estimated mass recoveries

Exp. No	C_o mg/L (clays) mol/L (tracer)	Flow Direction[a]	U_{tot} [b] (cm/min)	$U_{s(i)}$ [c] (cm/min)	D [b] (cm^2/min)	k_c [b] (1/min)	M_r (%)	$M_{1(c)}/M_{1(t)}$
KGa-1b								
1	62.8	H	0.73741±0.0018	0.00000	1.0614±0.098	0.0103±0.001	53.5	1.19
2	50.3	VU	0.73841±0.0008	-0.00159	0.2968±0.036	0.0236±0.001	32.6	1.05
3	67.6	VD	0.74193±0.0009	0.00193	0.5984±0.026	0.0037±0.001	79.5	1.12
4	56.6	DU	0.73474±0.0015	-0.00526	0.6790±0.063	0.0233±0.001	37.6	1.07
5	66	DD	0.74330±0.0016	0.00330	0.6554±0.052	0.0153±0.004	47.9	1.05
STx-1b								
6	100.1	H	0.73895±0.0004	0.00000	0.7377±0.052	0.0123±0.001	58.6	1.16
7	105.9	VU	0.73827±0.0016	-0.00174	0.5521±0.018	0.0164±0.001	65	0.89

8	102.3	VD	0.74219±0.0013	0.00219	0.5272±0.029	0.0033±0.001	93.8	1.01
9	75.9	DU	0.73264±0.0023	-0.00736	1.1751±0.094	0.0123±0.001	61.5	1.31
10	82.5	DD	0.74439±0.0026	0.00438	0.5157±0.072	0.0048±0.000	83.1	1.06
Tracer								
	0.01	H	0.74016±0.0001	–	0.1369±0.033		100	
	0.01	VU, VD	0.73985±0.0002	–	0.1671±0.041		100	
	0.01	DU, DD	0.73995±0.0001	–	0.1568±0.031		100	

[a] H-horizontal, VU-vertical up-flow, VD-vertical down-flow, DU-diagonal up-flow, DD-diagonal down-flow. [b] Fitted with ColloidFit. [c] Evaluated with equation (2).

ACKNOWLEDGMENTS

This research has been co-financed by the European Union (European Social Fund-ESF) and Greek National Funds through the Operational program "Education and Lifelong Learning" under the action Aristeia I (Code No. 1185).

REFERENCES

(1) Mills, W.B., S. Liu, and F.K. Fong, Literature review and model (COMET) for colloid/metals transport in porous media, Ground Water, 1991, 29, 199–208.
(2) Abdel-Salam, A., and C.V. Chrysikopoulos, Analysis of a model for contaminant transport in fractured media in the presence of colloids, J. Hydrol., 1995, 165, 261–281, doi:10.1016/0022-1694(94)02675-2.
(3) Ouyang, Y, D. Shinde, R.S. Mansell, and W. Harris, Colloid enhanced transport of chemicals in subsurface environments: a review, Crit. Rev. Environ. Sci. Technol., 1996, 26, 189–204.
(4) Harvey, R.W., and S.P. Garabedian, Use of colloid filtration theory in modeling movement of bacteria through a contaminated sandy aquifer, Environ. Sci. Technol., 1991, 25, 178–185.
(5) James, S. C.; and C. V. Chrysikopoulos, Analytical solutions for monodisperse and polydisperse colloid transport in uniform fractures. *Colloids Surf. A* 2003, *226*, 101–118, DOI 10.1016/S0927-7757(03)00316-9.
(6) Jin, Y.; Flury, M. Fate and transport of viruses in porous media. *Adv. Agronomy* 2002, *77*, 39–102.
(7) Keller, A. A.; Sirivithayapakorn, S. S.; Chrysikopoulos, C. V. Early breakthrough of colloids and bacteriophage MS2 in a water-saturated sand column. *Water Resour. Res.* 2004, *40*, W08304, DOI 10.1029/2003WR002676.
(8) James, S. C.; Bilezikjian, T. K.; Chrysikopoulos, C. V. Contaminant transport in a fracture with spatially variable aperture in the presence of monodisperse and polydisperse colloids. *Stoch. Environ. Res. Risk Assess.* 2005, *19* (4), 266–279, DOI 10.1007/s00477-004-0231-3.
(9) Tong, M.; Johnson, W. P. Excess colloid retention in porous media as a function of colloid size, fluid velocity, and grain angularity. *Environ. Sci. Technol.* 2006, *40*, 7725–7731.
(10) Harter, T.; Wagner, S.; Atwill, E. R. Colloid transport and filtration of *Cryptosporidium parvum* in sandy soils and aquifer sediments. *Environ. Sci. Technol.* 2000, *34*, 62–70.
(11) Xu, S.; Gao, B.; Saiers, J. E. Straining of colloidal particles in saturated porous media. *Water Resour. Res.* 2006, *42*, W12S16, DOI 10.1029/2006WR004948.
(12) Bradford, S. A.; Bettahar, M. Concentration dependent transport of colloids in saturated porous media. *J. Contam.* Hydrol. 2006, 82, 99–117.
(13) Ma, H.; Johnson, W. P. Colloid retention in porous media of various porosities: predictions by the hemispheres-in-cell model. Langmuir 2010, 26 (3), 1680–1687.
(14) Yoon, J. K.; Germaine, J. T.; Culligan, P. J. Visualization of particle behavior within a porous medium: mechanisms for particle filtration and retardation during downward transport. Water Resour. Res. 2006, 42, W06417, DOI 10.1029/2004WR003660.
(15) Xu, S.; Liao, Q.; Saiers, J. E. Straining of nonspherical colloids in saturated porous media. Environ. Sci. Technol. 2008, 42, 771–778.
(16) Shen, C.; Lazouskaya, V.; Zhang, H.; Wang, F.; Li, B.; Jin, Y.; Huang, Y. Theoretical and experimental investigation of detachment of colloids from rough collector surfaces. Colloids Surf. A 2012, 410, 98–110.
(17) Ryan, J. N.; Gschwend, P. M. Effects of ionic strength and flow rate on colloid release: relating kinetics to intersurface potential energy. *J. Colloid Intrerface Sci.* 1994, *164*, 21–34.
(18) Park, N., T.N. Blanford, and P.S. Huyakorn, VIRALT: A modular semi-analytical and numerical model for simulating viral transport in ground water, International Ground Water Modeling Center, Colorado School of Mines, Golden, CO, 1992.
(19) Basha, H. A.; Culligun, P. J. Modeling particle transport in downward and upward flows. *Water Resour. Res.* 2010, *46*, W07518, DOI 10.1029/2009WR008133.

(20) Chrysikopoulos, C. V.; Abdel-Salam, A. Modeling colloid transport and deposition in saturated fractures. *Colloids Surf. A: Physicochem. Eng. Aspects* 1997, *121*, 189−202, DOI 10.1016/S0927-7757(96)03979-9.
(21) Grolimund, D.; Borkovec, M. Release of colloidal particles in natural porous media by monovalent and divalent cations. *J. Contam. Hydrol.* 2006, *87*, 155–175.
(22) Tosco, T.; Tiraferri, A.; Sethi, R. Ionic strength dependent transport of microparticles in saturated porous media: modeling mobilization and immobilization phenomena under transient chemical conditions. *Environ. Sci. Technol.* 2009, *43*, 4425–4431.
(23) Kim, H. N.; Bradford, S. A.; Walker, S. L. *Escherichia coli* O157:H7 transport in saturated porous media: role of solution chemistry and surface macromolecules. *Environ. Sci. Technol*. 2009, *43*, 4340–4347.
(24) Wan, J.; Tokunaga, T.; Tsang, C. Bacterial sedimentation through a porous medium. *Water Resour. Res*. 1995, *31* (7), 1627–1636.
(25) Chen, G.; Hong, Y.; Walker, S. L. Colloidal and bacterial deposition: role of gravity. *Langmuir* 2010, *26* (1), 314–319.
(26) James, S. C.; Chrysikopoulos, C. V. Dense colloid transport in a bifurcating fracture. J. Colloid Interface Sci. 2004, 270, 250–254, DOI 10.1016/j.jcis.2003.09.033.
(27) Chrysikopoulos, C. V.; Syngouna, V. I. Attachment of bacteriophages MS2 and ΦX174 onto kaolinite and montmorillonite: extended-DLVO interactions. Colloids Surfaces B: Biointerfaces 2012, 92, 74–83, DOI 10.1016/j.colsurfb.2011.11.028.
(28) Ma, H.; Pazmino, E. F.; Johnson, W. P. Gravitational settling effects on unit cell predictions of colloidal retention in porous media in the absence of energy barriers. *Environ. Sci. Technol.* 2011, *45*, 8306–8312.
(29) Jin, Y.; Pratt, E.; Yates, M. Effect of mineral colloids on virus transport through saturated sand columns. *J. Environ. Qual*. 2000, *29*, 532–540.
(30) Vasiliadou, I. A.; Chrysikopoulos, C. V. Cotransport of *Pseudomonas putida* and kaolinite particles through water saturated columns packed with glass beads. *Water Resour. Res.* 2011, *47*, W02543, DOI 10.1029/2010WR009560.
(31) Syngouna, V. I.; Chrysikopoulos, C. V. Cotransport of clay colloids and viruses in water saturated porous media. *Colloids Surf. A: Physicochem. Eng. Aspects* 2013, *416*, 56–65, DOI 10.1016/j.colsurfa.2012.10.018.
(32) Katzourakis, V. E.; Chrysikopoulos, C. V. Mathematical modeling of colloid and virus cotransport in porous media: Application to experimental data, *Adv. Water Resour.* 2014, *68*, 62–73, DOI 10.1016/j.advwatres.2014.03.001.
(33) Silliman, S. E.; Dunlap, R.; Fletcher, M.; Schneegurt, M.A. Bacterial transport in heterogeneous porous media: observations from laboratory experiments. *Water Resour. Res.* 2001, *37* (11) 2699–2707.
(34) Chrysikopoulos, C. V.; Masciopinto, C.; La Mantia, R.; Manariotis, I. D. Removal of biocolloids suspended in reclaimed wastewater by injection in a fractured aquifer model. *Environ. Sci. Technol.* 2010, *44* (3), 971–977, DOI 10.1021/es902754n, 2010.
(35) Chrysikopoulos, C. V.; Syngouna, V. I.; Vasiliadou, I. A.; Katzourakis, V. E. Transport of *Pseudomonas putida* in a three-dimensional bench scale experimental aquifer. *Transport in Porous Media* 2012, *94*, 617–642, DOI 10.1007/s11242-012-0015-z.
(36) Thomas, J. M.; Chrysikopoulos, C. V. Experimental investigation of acoustically enhanced colloid transport in water-saturated packed columns. J. Colloid Interface Sci. 2007, 308 (1), 200–2007, DOI 10.1016/j.jcis.2006.12.062.
(37) Pruett, R. J.; Webb, H. L. Sampling and analysis of KGa-1b well-crystallized kaolin source clay. Clays Clay Miner. 1993, 41 (4) 514–519.
(38) Van Olphen, H.; Fripiat, J. J. Data Handbook for Clay Minerals and Other Non-metallic Minerals. Pergamon Press, Oxford, England, 346 pp, 1979.
(39) Sanders, R. L.; Washton, N. M.; Mueller, K. T. Measurement of the reactive surface area of clay minerals using solid-state NMR studies of a probe molecule. J. Phys. Chem. C 2010, 114 (12), 5491–5498.
(40) Rong, X.; Huanga, Q.; He, X.; Chen, H.; Cai, P.; Liang, W. Interaction of Pseudomonas putida with kaolinite and montmorillonite: A combination study by equilibrium adsorption, ITC, SEM and FTIR. Colloids Surf. B: Biointerfaces 2008, 64, 49–55.
(41) Sim, Y.; Chrysikopoulos, C. V. Three-dimensional analytical models for virus transport in saturated porous media. Transport in Porous Media 1998, 30, 87–112, DOI 10.1023/A:1006596412177.
(42) Chrysikopoulos, C. V.; Roberts, P. V.; Kitanidis, P. K. One-dimensional solute transport in porous media with partial well-to-well recirculation: Application to field experiments. Water Resour. Res. 1990, 26, 1189–1195, DOI 10.1029/89WR03629.
(43) Bolster, C. H.; Mills, A. L.; Hornberger, G. M.; Herman, J. S. Spatial distribution of diposited bacteria following miscible displacement experiments in intact cores. *Water Resour. Res.* 1999, *35* (6), 1797–1807.
(44) Compere, F.; Porel, G.; Delay, F. Transport and retention of clay particles in saturated porous media: influence of ionic strength and pore velocity. *J. Contam. Hydrol*. 2001, 49, 1–21.
(45) Schijven, J. F.; Hassanizadeh, S. M.; de Bruin, R. H. A. M. Two-site kinetic modeling of bacteriophages transport through columns of saturated dune sand. J. Contam. Hydrol. 2002, 57, 259–279.
(46) Sim, Y.; Chrysikopoulos, C. V., Analytical models for one-dimensional virus transport in saturated porous media. Water. Resour. Res. 1995, 31, 1429–1437, DOI 10.1029/95WR00199. (Correction, Water Resour. Res., 1996, 32, 1473, DOI 10.1029/96WR00675).

(47) Russel, W. B.; Saville, D. A.; Schowlter, W.R. Colloidal Dispersions, Cambridge University Press, Cambridge, UK, 525 pp., 1989.
(48) Tim, U.S. and S. Mostaghimi, Model for predicting virus movement through soils, Ground Water, 1991, 29(2), 251–259.